

# Dalton Transactions

Accepted Manuscript



This is an *Accepted Manuscript*, which has been through the RSC Publishing peer review process and has been accepted for publication.

*Accepted Manuscripts* are published online shortly after acceptance, which is prior to technical editing, formatting and proof reading. This free service from RSC Publishing allows authors to make their results available to the community, in citable form, before publication of the edited article. This *Accepted Manuscript* will be replaced by the edited and formatted *Advance Article* as soon as this is available.

To cite this manuscript please use its permanent Digital Object Identifier (DOI®), which is identical for all formats of publication.

More information about *Accepted Manuscripts* can be found in the [Information for Authors](#).

Please note that technical editing may introduce minor changes to the text and/or graphics contained in the manuscript submitted by the author(s) which may alter content, and that the standard [Terms & Conditions](#) and the [ethical guidelines](#) that apply to the journal are still applicable. In no event shall the RSC be held responsible for any errors or omissions in these *Accepted Manuscript* manuscripts or any consequences arising from the use of any information contained in them.

Cite this: DOI: 10.1039/c0xx00000x

www.rsc.org/xxxxxx

## ARTICLE TYPE

## Luminescent gels by self-assembling platinum complexes

Naveen Kumar Allampally,<sup>a,b</sup> Cristian A. Strassert,<sup>\*a</sup> Luisa De Cola<sup>\*a</sup>

Received (in XXX, XXX) Xth XXXXXXXXX 20XX, Accepted Xth XXXXXXXXX 20XX

DOI: 10.1039/b000000x

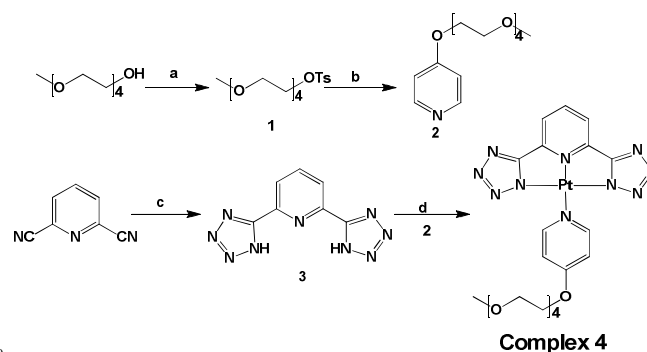
A platinum complex bearing a tetraethyleneglycol chain has been designed and its self-assembly properties investigated. In solution, only a yellow phosphorescence of the aggregated species is observed. The complex gives luminescent gels of different colours with DCM and DMF, reaching up to 60% photoluminescence quantum yield.

## Introduction

Square planar Pt(II) complexes are known for their phosphorescence and long-lived excited states, as well as for their tendency to stack and form aggregates in which metal-metal interactions influence their photophysical properties.<sup>1-5</sup> The switching of metal-metal interactions by external stimuli such as solvent, anions and heating has been explored, for instance, by Yam et al., employing cationic terpyridinechelates.<sup>6-8</sup> These interactions can lead to the gelation of organic solvents or water. There has been considerable interest in polymer gels as potential carriers for drug delivery.<sup>9,10</sup> However, issues related to their biodegradability, chemical composition and uncontrollable disassembly limit their applications.<sup>11</sup> Low molecular weight gelators (LMWG), on the other hand, use non-covalent assembling processes based on H-bonding and  $\pi$ - $\pi$  stacking, as well as metallophilic,<sup>12</sup> van der Waals, hydrophobic and hydrophilic interactions.<sup>13</sup> Their switchable sol-gel transition triggered by external stimuli such as temperature, pH,<sup>14</sup> anions,<sup>15</sup> metal ions<sup>16</sup> and ultrasound<sup>17</sup> facilitate their application in sensors<sup>18</sup> and biomedical research.<sup>19</sup> Moreover, it is possible to chemically modify the properties of the gelator, and to have a defined control of the composition and the morphology.<sup>11</sup> Indeed assemblies vs single chromophores can have several advantages. For examples new emerging properties for organometallic soft assemblies as enhanced luminescence, energy change of the emissive excited state, resulting by electronic interactions, or energy hopping between the chromophores can be observed. The extent of aggregation and therefore of the properties rising from the interactions can be controlled by the chelating chromophoric or by the ancillary ligand(s) leading to secondary interactions such as  $\pi$ - $\pi$  or metal-metal interactions upon formation of the assembly.<sup>16-22</sup> Furthermore, such aggregates, when luminescent can be potentially employed for OLED devices<sup>23,24</sup> and sensors.<sup>25</sup> We have recently shown that neutral Pt(II) complexes bearing a tridentate, dianionic chelate and a substituted pyridine ligand can assemble into filaments and gels displaying a bright yellow luminescence, which can be monitored with high sensitivity along the aggregation process. In dilute fluid solutions

at room

temperature, however, no emission was observed from the monomeric units. In frozen matrices at 77K, and due to the strong tendency of the molecular species to form luminescent aggregates, we were not able to see the emission of the monomers.<sup>23</sup> Herein we report a strategy to design and synthesize platinum complexes that enabled us to control the degree of aggregation in polar solvents by the insertion of a tetraethyleneglycol (PEG) chain (Scheme 1). The resulting complex **4** showed the characteristic yellow phosphorescence of the aggregated species, in solution and also the emission of the monomeric species at low temperature. Furthermore complex **4** is able to form reversible DCM and DMF luminescent gels (Figure 1).



**Scheme 1** Synthesis of complex 4. a) KOH, TsCl, DCM, 5h, below 5 °C (94% yield); b) 4-hydroxypyridine, K<sub>2</sub>CO<sub>3</sub>, ACN, reflux, 48 h (75% yield); c) NaCN, AcOH, n-butanol, reflux d) Pt(DMSO)<sub>2</sub>Cl<sub>2</sub>, DIPEA, ACN, reflux overnight (67% yield)

## Experimental section

**Materials:** All reagents were used without further purification, as supplied by Fluka or Sigma Aldrich. Tetraethyleneglycol monomethyl ether and tosyl chloride were purchased from Acros Organics, and 4-hydroxypyridine from Alfa Aesar. Spectroscopic grade solvents were purchased from Merck.

**Instrumentation:** NMR spectra were recorded with a Bruker

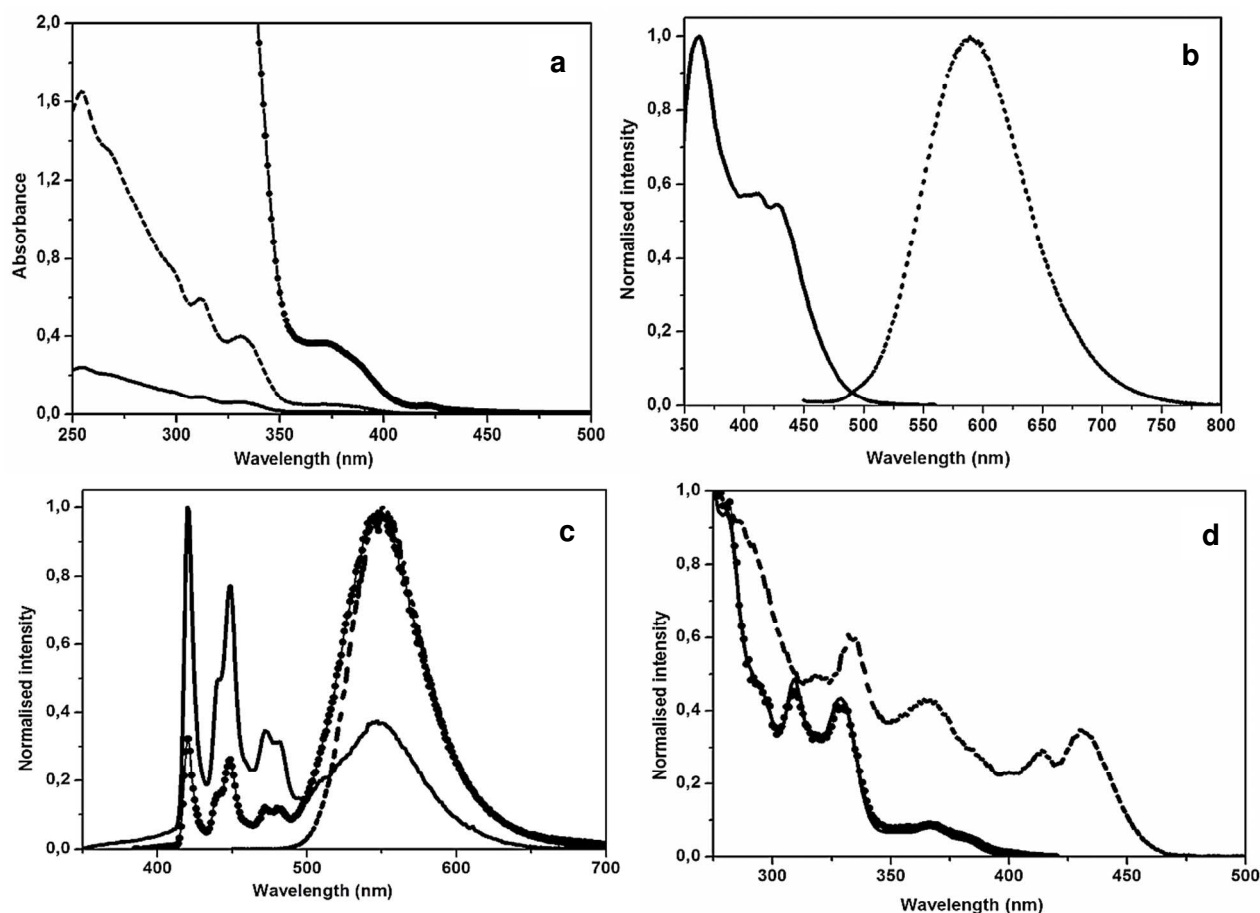


**Fig. 1:** a) Absorption spectra of complex **4** in DCM at room temperature (solid line:  $5 \times 10^{-6}$  M; dashed line:  $5 \times 10^{-5}$  M; dotted line:  $5 \times 10^{-4}$  M). b) Excitation (solid line,  $\lambda_{em} = 590$  nm) and emission (dashed line,  $\lambda_{ex} = 430$  nm) of complex **4** in DCM at room temperature ( $5 \times 10^{-4}$  M). c) Emission spectra of complex **4** at 77 K in frozen 2-MTHF glass (solid line:  $\lambda_{ex} = 330$  nm; circle line:  $\lambda_{ex} = 385$  nm; dashed line:  $\lambda_{ex} = 430$  nm). d) Excitation spectra of complex **4** at 77 K in frozen 2-MTHF glass (solid line:  $\lambda_{em} = 420$  nm; circle line:  $\lambda_{em} = 450$  nm; dashed line:  $\lambda_{em} = 540$  nm).

AMX400 and a Bruker ARX300 spectrometers. Chemical shifts were referred to the peak of the residual protic solvent existing in the deuterated solvent. The UV-Vis absorption spectra were recorded on a Cary 5000 UV-Vis-NIR spectrophotometer and were baseline and solvent corrected. Steady-state luminescence experiments were performed with a Spex FluoroLog-3 spectrofluorometer (Horiba-Jobin-Yvon Inc.) equipped with a TBX detector and double-grating excitation and emission monochromators (2.1 nm/mm dispersion; 1200 grooves/mm). The emission spectra were corrected for monochromator and detector efficiency and for the light source intensity (450W xenon lamp), employing standard correction files and recording the reference signal. Time resolved measurements were performed using the time-correlated single-photon counting (TCSPC) option on the Spex FluoroLog-3. NanoLED (431 nm; FWHM < 200 ps) with repetition rates between 10 kHz and 1 MHz was used to excite the samples. The excitation sources were mounted directly on the sample chamber at 90° to the detector. The photons collected are correlated by a time-to-amplitude converter (TAC) to the S3 excitation pulse. Signals were collected using an IBH DataStation Hub photon counting module, and data analysis was performed using the commercially available DAS6 software

(HORIBA JobinYvon IBH). The goodness of fit was assessed by minimizing the reduced chi squared function ( $\chi^2$ ) and visual inspection of the weighted residuals. Luminescence quantum yields were measured with a Hamamatsu Photonics absolute PL quantum yield measurement system (C9920-02) equipped with a L9799-01 CW xenon light source (150 W), monochromator, C7473 photonic multichannel analyzer, and integrating sphere, and employing U6039-05 photoluminescence quantum yield (PLQY) measurement software (Hamamatsu Photonics, Ltd., Shizuoka, Japan). For the acquisition of SEM images, the sol of the respective gels samples was drop-casted on the glass slide. After gelation and evaporation of the solvent, the samples were covered by a 5 nm thick silver layer, and finally investigated using a Zeiss 1540 EsB dual beam focused ion beam/field emission scanning electron microscope. Fluorescence microscope images were recorded on an Olympus BX51 using a 100x oil immersion objective (Planapochromat, NA 1.4) and an Olympus U-MWBV2 excitation cube; images were recorded on a XC-10 colour camera (Olympus).

Cite this: DOI: 10.1039/c0xx00000x

www.rsc.org/xxxxxx

ARTICLE TYPE

Table 1. Photophysical properties of complex 4

Sample	$\lambda_{em}$ [nm]	$^f \phi \times 100$	$^g \tau$ [μs]	$^h$ CGC [mg/mL]
<sup>a</sup> DCM, RT	590	-	0.19 (53.09%), 0.49 (46.91%)	-
<sup>b</sup> DCM, RT	590	-	0.21 (53.93%), 0.49 (46.06%)	-
<sup>c</sup> 2-MTHF, 77K	540	-	2.71(86.91%), 10.19 (13.09%)	-
<sup>d</sup> 2-MTHF, 77K	420	-	5.34 (13.05%), 15.05 (86.95%)	-
<sup>e</sup> 2-MTHF, 77K	540	-	3.15 (84.19%), 13.43(15.81%)	-
DCM gel	550	7.5	0.506	8
DMF gel	515	60	0.22(54.79%), 0.57(45.21%)	7.8
Fibers	550	<sup>i</sup> 7.4	0.25	-
Neat film	550	7.1	0.28	-

<sup>a</sup>deacrated; <sup>b</sup>aerated; <sup>c</sup> glassy matrix,  $\lambda_{ex}$  = 431 nm,  $\lambda_{em}$  = 540 nm; <sup>d</sup>  $\lambda_{ex}$  = 337 nm,  $\lambda_{em}$  = 420 nm; <sup>e</sup>  $\lambda_{ex}$  = 337 nm,  $\lambda_{em}$  = 540 nm; <sup>f</sup> average value between  $\lambda_{ex}$  = 365 and  $\lambda_{ex}$  = 425 nm; <sup>g</sup> relative amplitudes are given in brackets; <sup>h</sup> critical gelation concentration (CGC, minimum amount of gelator required for 1mL of solvent; <sup>i</sup>  $\lambda_{ex}$  = 455 nm.

5 General synthetic procedure

Compounds Pt(DMSO)<sub>2</sub>Cl<sub>2</sub>,<sup>26</sup> 2,6 bis-tetrazole-5-yl-pyridine,<sup>27</sup> 4(2,5,8,11-tetraoxatridecan-13-yloxy)pyridine<sup>28</sup> and 2,5,8,11-tetraoxatridecan-13-yl 4-methyl benzene- sulfonate<sup>29</sup> were synthesized and purified according to literature procedures.

2,5,8,11-tetraoxatridecan-13-yl-14-methyl- benzenesulfonate (**1**), 4-(2,5,8,11-tetraoxatridecan-13-yl-oxy)pyridine (**2**) and complex **4** were synthesized as described below.

**Synthesis of 2,5,8,11-tetraoxatridecan-13-yl-14-methyl-benzenesulfonate (1):** Tetraethylene glycol mono-methyl ether (1041 mg, 1 eq.) and p-toluenesulfonyl chloride (1001mg, 1.05eq.) were dissolved in DCM and powdered KOH (1122mg, 2 eq.) was added slowly to this mixture at 0° C. After stirring for 5 h (below 5° C), the reaction mixture was quenched with water. The product was extracted into DCM, which was washed with brine and dried over MgSO<sub>4</sub>. The product was used without further purification. Yield: 1702 mg, 94%. <sup>1</sup>H NMR (300 MHz, CDCl<sub>3</sub>) δ 7.76 – 7.66 (m, 2H), 7.32 – 7.23 (m, 2H), 4.15 – 4.01 (m, 2H), 3.61 (dd, *J* = 5.4, 4.2 Hz, 2H), 3.58 – 3.43 (m, 12H), 3.29 (s, 3H), 2.37 (s, 3H); <sup>13</sup>C NMR (75 MHz, CDCl<sub>3</sub>) δ 151.42 , 139.55 , 136.44 , 134.54 , 84.04 (d, *J* = 32.1 Hz), 83.40 , 78.49 , 75.90 , 75.23 , 65.59 , 28.23; HRMS (ESI) *m/z*: calculated, 385.1291 [M + Na]<sup>+</sup>; found, 385.1289[M + Na]<sup>+</sup>

**Synthesis of 4-(2,5,8,11-tetraoxatridecan-13-yl-oxy)pyridine (2):** 2,5,8,11-tetraoxatridecan-13-yl 4-methylbenzenesulfonate (1631mg, 1 eq.), K<sub>2</sub>CO<sub>3</sub>(684mg, 1.1 eq.) and 4-hydroxy pyridine (428mg, 1eq.) were taken in dry acetonitrile (ACN) and the reaction mixture was refluxed for 48 h under N<sub>2</sub>. The ACN was removed under reduced pressure. To this crude reaction mixture, water and DCM were added and the product was extracted into

DCM, which was washed with brine and dried over MgSO<sub>4</sub>. The product was further purified by silica gel column chromatography using 5% MeOH in DCM as eluent. Yield: 963 mg, 75%. <sup>1</sup>H NMR (300 MHz, CDCl<sub>3</sub>) δ 8.38 (d, *J* = 5.3 Hz, 2H), 6.79 (dd, *J* = 4.8, 1.5 Hz, 2H), 4.14 (dd, *J* = 5.4, 4.1 Hz, 2H), 3.84 (dd, *J* = 5.4, 4.1 Hz, 2H), 3.71 – 3.58 (m, 11H), 3.53 – 3.48 (m, 2H), 3.34 (d, *J* = 2.1 Hz, 3H); <sup>13</sup>C NMR (75 MHz, CDCl<sub>3</sub>) δ 171.36 , 157.58 , 116.90 , 83.88 (d, *J* = 32.0 Hz), 83.24 , 78.48 , 75.86 , 73.78 , 65.58; HRMS (ESI) *m/z*: calculated, 286.1649 [M + H]<sup>+</sup>; found, 286.1650 [M + H]<sup>+</sup>, 308.1471 [M + Na]<sup>+</sup>

**Synthesis of complex 4:** 4-(2,5,8,11-tetraoxatridecan-13-yloxy)pyridine (285mg, 1 eq.), 2,6-di(1H-tetrazol-5-yl)pyridine (215mg, 1 eq.) and diisopropylethylamine(418 μL, 2.4 eq.) were added into an ACN solution containing Pt(DMSO)<sub>2</sub>Cl<sub>2</sub>(422 mg, 1 eq.). Initially the reaction mixture was sonicated to dissolve the solids and then refluxed under N<sub>2</sub> for 12 hours. The product was filtered off, washed with water, and purified by running a column using silica gel and 5% MeOH in DCM as eluent. Yield: 465 mg, 67%. <sup>1</sup>H NMR (300 MHz, CD<sub>2</sub>Cl<sub>2</sub>) δ 9.47 (d, *J* = 7.2 Hz, 2H), 8.23 (dd, *J* = 8.4, 7.2 Hz, 1H), 8.06 (d, *J* = 7.6 Hz, 2H), 7.12 (d, *J* = 7.2 Hz, 2H), 4.45 – 4.34 (m, 2H), 4.01 – 3.89 (m, 2H), 3.76 – 3.69 (m, 2H), 3.68 – 3.55 (m, 8H), 3.50 (ddd, *J* = 9.1, 4.7, 3.2 Hz, 2H), 3.33 (s, 3H); HRMS (ESI) *m/z*: calculated, 716.1628 [M + Na]<sup>+</sup>; Found, 716.1614[M + Na]<sup>+</sup>, 694.1793[M + H]<sup>+</sup>, CHN Analysis: Calculated (**4** + CH<sub>3</sub>CN), C, 37.60 %; H, 3.98 %; N, 20.97 %; Found, C, 37.54 %; H, 3.94 %; N, 18.74 %

Results and discussion

The room temperature absorption spectra of complex **4** in DCM display a pyridine- and a tridentate-ligand-centred (<sup>1</sup>LC) π-π\*

Cite this: DOI: 10.1039/c0xx00000x

www.rsc.org/xxxxxx

## ARTICLE TYPE

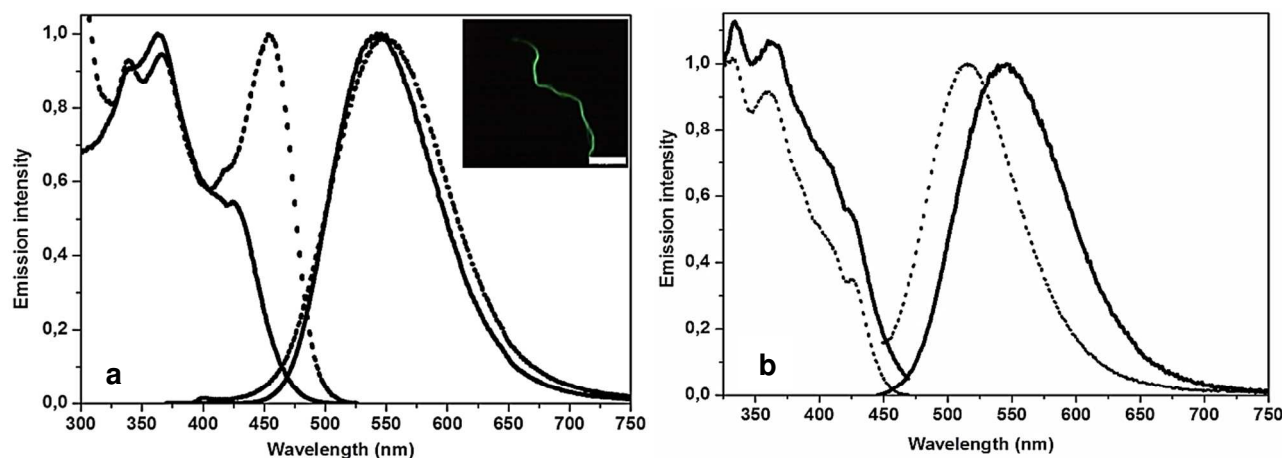


**Fig. 2:** a) Excitation (left solid line,  $\lambda_{em}=550$  nm) and emission (right solid line,  $\lambda_{ex}=340$  nm) spectra of a neat film of complex 4. Excitation (left dashed line,  $\lambda_{em}=550$  nm) and emission (right dashed line,  $\lambda_{ex}=340$  nm) of fibers of complex 4. Inset: Fluorescence microscopy image of a single fiber. Scale bar: 20  $\mu$ m. b) Luminescence of gels of complex 4. DCM gel: excitation (left solid line,  $\lambda_{em}=550$  nm) and emission (right solid line,  $\lambda_{ex}=425$  nm) spectra. DMF gel: excitation (left dotted line,  $\lambda_{em}=510$  nm) and emission (right dotted line,  $\lambda_{ex}=425$  nm) spectra.

transition (310 nm and 340 nm, respectively), as well as a characteristic metal to ligand charge transfer ( $^1$ MLCT) band (360 nm - 400 nm, Figure 1a). Above  $10^{-4}$  M, the solutions also show an incipient band around 420 nm. This observation points towards ground state aggregation and electronic coupling (Figure 1a), giving rise to a metal-metal to ligand charge transfer band ( $^1$ MMLCT). Indeed, plotting the absorption spectra at different concentrations reveals that Lambert-Beer's law is not followed (see supplementary information FigureS1). In dilute DCM solutions of complex 4 (below  $10^{-4}$  M), no emission is observed at any excitation wavelength. Above  $10^{-4}$  M, however, complex 4 displays a weak yellow luminescence (Table 1 and Figure 1b), which can be assigned to the metal-metal to ligand charge transfer state ( $^3$ MMLCT) of aggregated species. In DMF, no measurable emission can be traced, even above  $10^{-3}$  M, thus indicating that the solvation capacity of the polar solvent overcomes the aggregation tendency. The concentration and solvent dependences of the absorption and emission spectra are indicative of aggregation equilibria leading to metal-metal interactions between the stacking complexes.<sup>23</sup> The excitation spectrum Figure 1b confirms this assignment, since the band around 430 nm appears relatively stronger, if compared with the absorption spectra (Figure 1a). Concentration-dependent  $^1$ HNMR experiments confirm the aggregation process, which shifts the aromatic signals to higher fields (see supplementary information FigureS2). At room temperature, the emission and excitation spectra do not depend on the excitation or emission wavelengths, respectively. At 77K, however, in 2-MTHF glassy matrices, a dual luminescence is observed (Figure 1c). Excitation in the UV (330 nm) originates a predominant deep-blue emission (420 nm) with a clear vibrational progression, which can be assigned to the phosphorescence from the metal-perturbed ligand-centred excited

triplet state ( $^3$ LC) of the monomeric species, as well as a weaker, unstructured luminescence ( $^3$ MMLCT, 540 nm) resembling the room temperature spectra of the aggregates. Indeed, the excited state lifetimes confirm these assignments (Table 1). Monitoring the emission at 420 nm, the long-lived  $^3$ LC state ( $\sim 15$   $\mu$ s) is obtained. At 540 nm, the emission decay shows a shorter-lived  $^3$ MMLCT state ( $\sim 3$   $\mu$ s). If compared with analogous Pt(II) complexes bearing 1,2,4-triazoles,<sup>30</sup> the greenligand centred luminescence appears shifted into the deep blue region of the electromagnetic spectrum. This is due to the lower HOMO level related to the tetrazole rings, as compared to the 1,2,4-triazoles, thus leading to a wider HOMO-LUMO gap. On the other hand, increasing the excitation wavelength inverts the relative intensities of the emission bands (Figure 1c), since the absorption of the aggregates becomes predominant, as can be observed in the excitation spectra monitoring at different emission wavelengths (Figure 1d).

In order to further confirm that the yellow emission is originated by aggregated species, we prepared fibers of complex 4 by pouring a DCM solution into cyclohexane. The resulting suspension of bundled filaments was deposited onto a microscope cover slip and analyzed on the fluorescence spectrometer and under the fluorescence microscope. For comparison, a DCM solution of complex 4 was directly drop-casted onto a glass slide and analyzed. Excitation and emission spectra of the fibers (Figure 2a), which are essentially self-assembled filaments composed of aggregates, show the same type of unstructured yellow emission profile as the drop-casted film. The excited state lifetimes of the filaments and the film present monoexponential decays and comparable PLQYs (Table 1). The fact that the excited state lifetimes are monoexponential, as opposed to the biexponential decays in solution, is due to the inherent rigidity



of the solid state, and also accounts for the blue shifted emission (Table 1). A similar rigido-solvatochromic effect is observed at

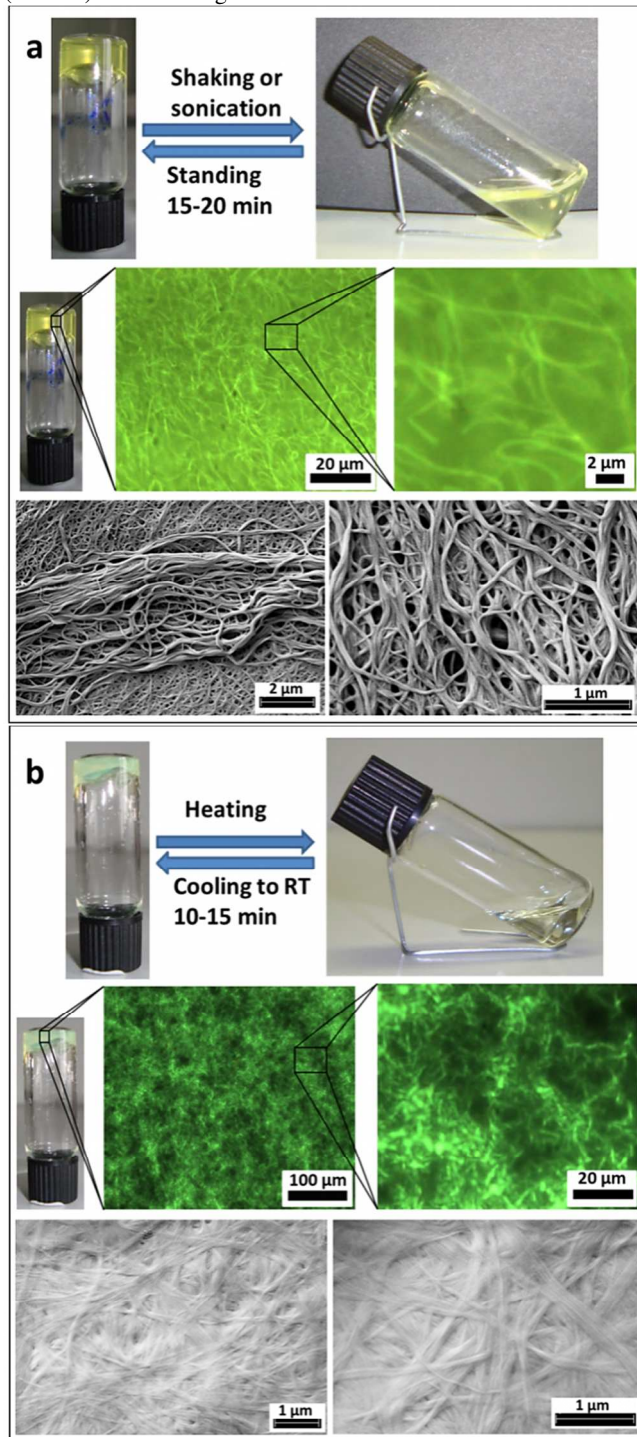


**Fig. 3.** a) DCM and b) DMF gels of complex **4**. Reversible gelation process (top), fluorescence microscope images (centre) and SEM images (bottom).

77K, as compared to room temperature (Table 1). Due to its fibre formation capacity, we further decided to investigate the gelating ability of complex **4**. Thus, the critical gelation concentration (CGC) was determined in DCM and DMF (Table 1). Complex **4** is able to gelate DCM and DMF at 8 mg/mL. The DCM can be gelated by dissolving the complex and leaving the

solution for 15 minutes at room temperature. The gel collapses into sol by shaking or sonication (Figure 3a). The DMF gel was obtained by dissolving the complex **4** in DMF at 60°C, and allowing the solution to cool down to room temperature. The stable gel can be reverted to the sol phase (Figure 3b) by gently heating to 60°C. Both gels are photoluminescent under UV light excitation, whereas the sols are not emissive at all in the same conditions. All the gels present the characteristic <sup>1</sup>MMLCT excitation bands around 430 nm (Figure 2b). The DCM gel shows a broad emission maximum at 550 nm (Figure 2b), displaying monoexponential lifetimes and a PLQY that resemble the drop casted film (Table 1). Contrastingly, the DMF gel emits with a broad band centred at 515 nm (Figure 2b and Table 1) showing a biexponential lifetime, and reaches the highest PLQY (60%). The surface morphology of DCM and DMF gels point towards an entanglement of the fibres, leading to a 3D-network encapsulating the solvent. The SEM and fluorescence microscopy images of the DCM gel show bundles of fibres with micrometer length and 50 nm – 100 nm width. The DMF gel displays particularly straight fibres (Figure 3). As previously mentioned, complex **4** is strongly solvated by DMF and therefore we assume that the corresponding gel involves a less pronounced Pt-Pt interaction. The weaker d-d orbital coupling originates a blue shift, showing that several parameters can be adjusted to tune the emission properties. Interestingly, a high PLQY accompanies the gelation of the most polar solvent, namely DMF. The different emission quantum yields could rise from the particular solvation of the polar PEG tail and the apolar chromophoric part. Indeed, we expect the Pt(II) centre to interact stronger with the apolar DCM, whereas the polar chains entangle in order to reduce their exposure to the solvent, thus bundling on the same side. On the other hand, in DMF, the Pt-Pt interactions are less pronounced due to the solvation of the polar PEG chains, thus preventing a closer approach of the metal centres. Consequently, the PEG chains could adopt an alternating configuration that favours a longer range order and increases the emission quantum yield.

## Conclusions

In conclusion, we have tuned the packing properties of a tridentate Pt(II) complex by inserting a polar PEG chain on the ancillary pyridine ligand. It enabled us to simultaneously monitor the spectroscopic properties of the monomeric (deep-blue luminescence) and aggregated (yellow phosphorescence) species. In particular, we have shown that the polarity of the solvent determines the extent of interaction within the aggregates and the gels, thus tuning the color and the PLQY of the assemblies.

## Acknowledgements

N. K. Allampally acknowledges Graduate School of Chemistry (GSC-MS, NRW) for doctoral fellowship.

## Notes and references

- <sup>65</sup> <sup>a</sup>CeNTech – Physikalisches Institut – Westfälische Wilhelms-Universität Münster, <sup>b</sup>Graduate School of Chemistry (GSC-MS)-Münster Heisenbergstr. 11, D-48149 Münster, Germany

View Online

E-mail: [decola@uni-muenster.de](mailto:decola@uni-muenster.de)

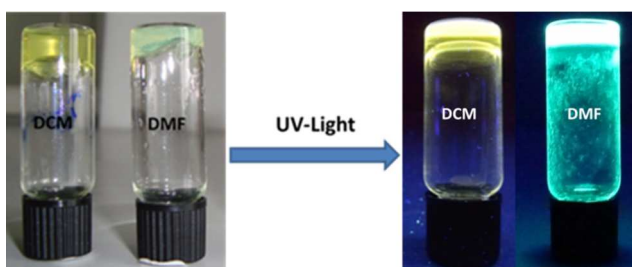
† Electronic Supplementary Information (ESI) available: Lambert-Beer's law plot and NMR spectra. See DOI: 10.1039/b000000x/

1. J. Schneider, P. Du, X. Wang, W. W. Brennessel, R. Eisenberg, *Inorg. Chem.*, 2009, **48**, 1498-1506; P. Jarosz, K. Lotito, J. Schneider, D. Kumaresan, R. Schmehl, and R. Eisenberg, *Inorg. Chem.*, 2009, **48**, 2420-2428; J. Schneider, P. Du, P. Jarosz, T. Lazarides, X. Wang, W. W. Brennessel and R. Eisenberg, *Inorg. Chem.*, 2009, **48**, 4306-4316.
2. J. A. G. Williams, *Top. Curr. Chem.*, 2007, **281**, 205-268 J. A. G. Williams, *Chem. Soc. Rev.*, 2009, **38**, 1783-1801; J. Kalinowski, V. Fattori, M. Cocchi and J. A. G. Williams, *Coord. Chem. Rev.*, 2011, **255**, 2401-2425.
3. F. N. Castellano, I. E. Pomestchenko, E. Shikhova, F. Hua, M. L. Muro and N. Rajapakse, *Coord. Chem. Rev.*, 2006, **250**, 1819-1828.
4. A. A. Rachford, F. Hua, C. J. Adams and F. N. Castellano, *Dalton Trans.*, 2009, 3950-3954; Y. Unger, A. Zeller, M. A. Taige, and T. Strassner, *Dalton Trans.*, 2009, 4786-4794.
5. B. Ma, P. I. Djurovich and M. E. Thompson, *Coord. Chem. Rev.* 2005, **249**, 1501-1510; B. Ma, P. I. Djurovich, S. Garon, B. Alleyne and M. E. Thompson, *Adv. Fun. Mater.*, 2006, **16**, 2438-2446
6. S. D. Cummings, *Coord. Chem. Rev.* 2009, **253**, 449-478.; R. McGuire, M. C. McGuire and D. R. McMillin, *Coord. Chem. Rev.*, 2010, **254**, 2574-2583.
7. K. M. C. Wong and V. W. W. Yam, *Acc. Chem. Res.*, 2011, **44**, 424-434.
8. V. W. W. Yam, K. H. Chan, K. M. C. Wong and N. Zhu, *Chem. Eur. J.*, 2005, **11**, 4535-4543.
9. V. W. W. Yam, K. H. Chan, K. M. C. Wong and B. W. Chu, *Angew. Chem. Int. Ed.*, 2006, **45**, 6169-6173.
10. Y. Q. Liang, Y. Qiao, S. T. Guo, L. Wang, C. P. Xie, Y. L. Zhai, L. D. Deng and A. J. E. Dong, *Soft Matter*, 2010, **6**, 1915-1922.
11. M. H. Park, M. K. Joo, B. G. Choi and B. Jeong, *Acc. Chem. Res.*, 2011.
12. W. T. Truong, Y. Su, J. T. Meijer, P. Thordarson and F. Braet, *Chem. Asian. J.*, 2011, **6**, 30-42.
13. F. Fages, *Angew Chem Int Ed Engl*, 2006, **45**, 1680-1682.
14. A. Dawn, T. Shiraki, S. Haraguchi, S. Tamaru and S. Shinkai, *Chem. Asian. J.*, 2011, **6**, 266-282; X. Y. Liu, *Top. Curr. Chem.*, 2005, **256**, 1-37; M. Žinic, F. Vögtle, F. Fages, *Top. Curr. Chem.*, 2005, **256**, 39-76; F. Fages, F. Vögtle, M. Žinic, *Top. Curr. Chem.*, 2005, **256**, 77-131
15. N. L. Fletcher, C. V. Lockett and A. F. Dexter, *Soft Matter*, 2011, **7**, 10210-10218.
16. G. O. Lloyd and J. W. Steed, *Nat. Chem.*, 2009, **1**, 437-442.
17. A. Kishimura, T. Yamashita and T. Aida, *J. Am. Chem. Soc.*, 2004, **127**, 179-183; C. A. Strassert, M. Mauro and L. De Cola, Photophysics of soft and hard molecular assemblies based on luminescent complexes, *Adv. Inorg. Chem.*, 2011, **63**, 47
18. L. Sambri, F. Cucinotta, G. De Paoli, S. Stagni, L. De Cola *New. J. Chem.* **2010**, **34**, 2093-2096. N. Komiya, T. Muraoka, M. Iida, M. Miyana, K. Takahashi and T. Naota, *J. Am. Chem. Soc.*, 2011, **133**, 16054-16061.
19. M.-O. M. Piepenbrock, N. Clarke and J. W. Steed, *Langmuir*, 2009, **25**, 8451-8456.
20. A. R. Hirst, B. Escuder, J. F. Miravet and D. K. Smith, *Angew. Chem. Int. Ed.*, 2008, **47**, 8002-8018.
21. A. Y. Tam, K. M. C. Wong, N. Zhu, G. Wang and V. W. W. Yam, *Langmuir*, 2009, **25**, 8685-8695.
22. F. Camerel, R. Ziessel, B. Donnio, C. Bourgogne, D. Guillon, M. Schmutz, C. Iacovita and J. P. Bucher, *Angew. Chem. Int. Ed.*, 2007, **46**, 2659-2662.
23. G. De Paoli, Z. Džolic, F. Rizzo, L. De Cola, F. Vögtle, W. M. Müller, G. Richardt and M. Žinic, *Adv. Fun. Mater.*, 2007, **17**, 821-828. M. Mauro, G. De Paoli, M. Otter, D. Donghi, G. D'Alfonso, L. De Cola *Dalton Trans.* **2011**, **40**, 12106-12116.
24. C. A. Strassert, C. H. Chien, M. D. G. Lopez, D. Kourkoulos, D. Hertel, K. Meerholz and L. De Cola, *Angew. Chem. Int. Ed.*, 2011, **50**, 946-950; A. Y. Tam, D. P. Tsang, M. Y. Chan, N. Zhu and V. W. W. Yam, *Chem Commun (Camb)*, 2011, **47**, 3383-3385.
25. J. Kalinowski, M. Cocchi, L. Murphy, J. A. G. Williams and V. Fattori, *Chem. Phys.*, 2010, **378**, 47-57.

25. V. W. W. Yam and K. M. C. Wong, *Chem. Commun.*, 2011, **47**, 11579-11592.
26. R. Romeo, L. M. Scolaro, V. Catalano and S. Achar, in *Inorganic Syntheses*, John Wiley & Sons, Inc., 2007, pp. 153-158.
27. J. M. Mcmanus and R. M. Herbst, *J. Org. Chem.*, 1959, **24**, 1462-1464.
28. A. Bouzide and G. Sauve, *Org. Lett.*, 2002, **4**, 2329-2332.
29. K. M. Bonger, R. J. van den Berg, L. H. Heitman, I. J. AP, J. Oosterom, C. M. Timmers, H. S. Overkleef and G. A. van der Marel, *Bioorg. Med. Chem.*, 2007, **15**, 4841-4856.
30. M. Mydlak, M. Mauro, F. Polo, M. Felicetti, J. Leonhardt, G. Diener, L. De Cola and C. A. Strassert, *Chem. Mater.*, 2011, **23**, 3659-3667.

## Table of contents

### Gelating organic solvents with a tailored phosphorescent Pt(II) complex



Supplementary Information

Luminescent gels by self-assembling platinum complexes

Naveen Kumar Allampally, Cristian A. Strassert\*, Luisa De Cola\*

Received (in XXX, XXX) Xth XXXXXXXXXX 20XX, Accepted Xth XXXXXXXXXX 20XX  
DOI: 10.1039/b000000x

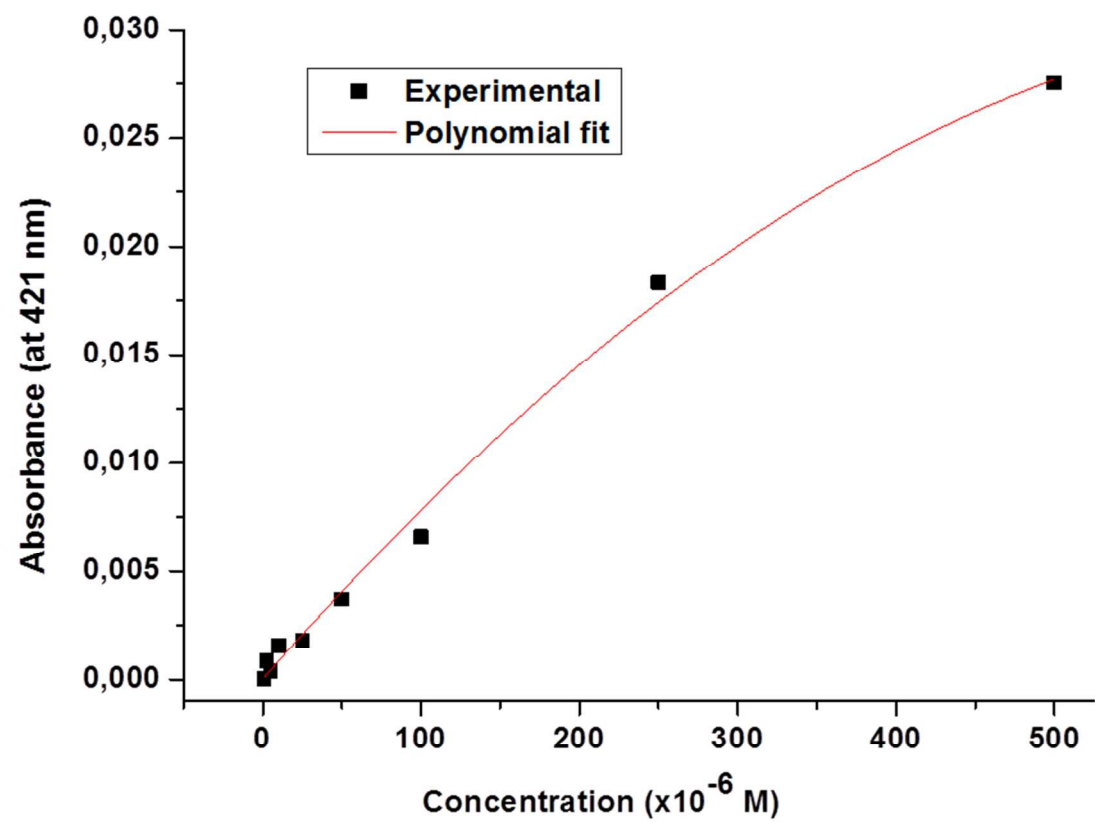
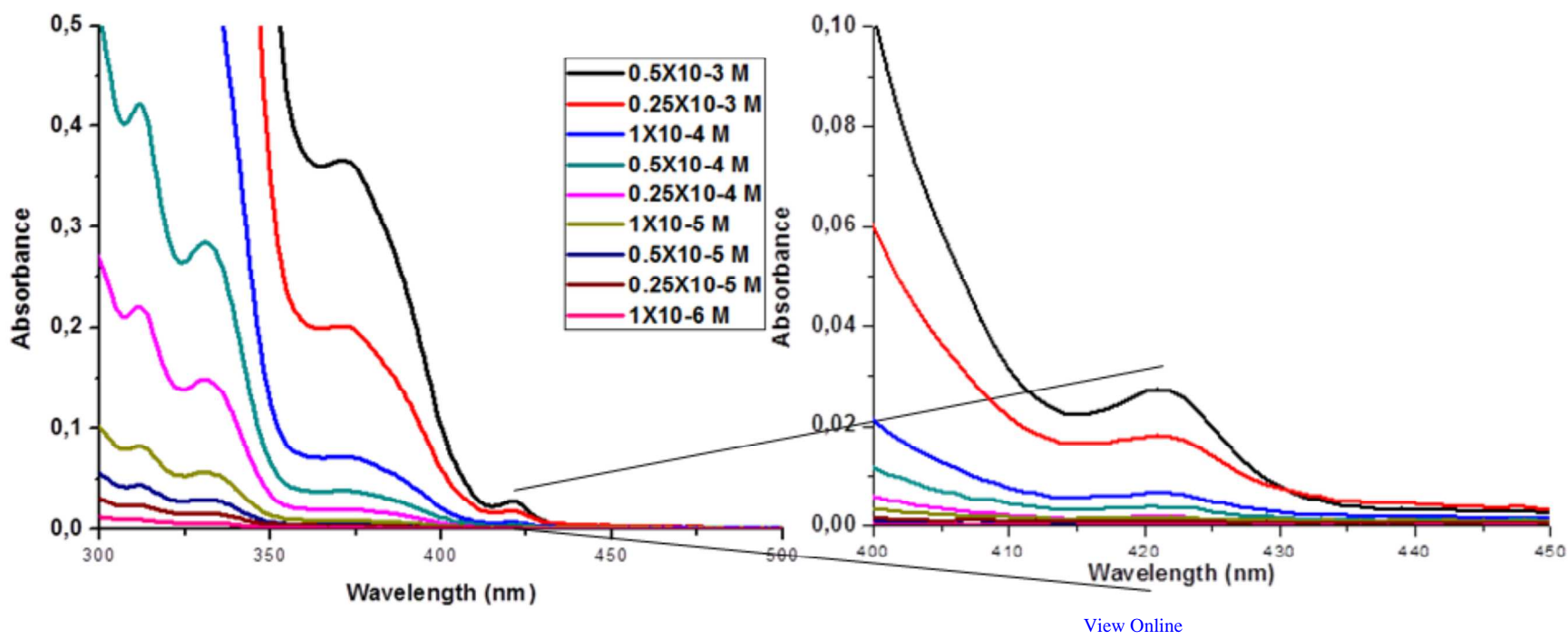


**Figure S1.** Absorption spectra at different concentration in dichloromethane solution of complex **4** (notice the concentration dependent<sup>1</sup>MMLCT band at 420 nm) (top). Plot of the absorbance vs concentration for complex **4** (bottom).



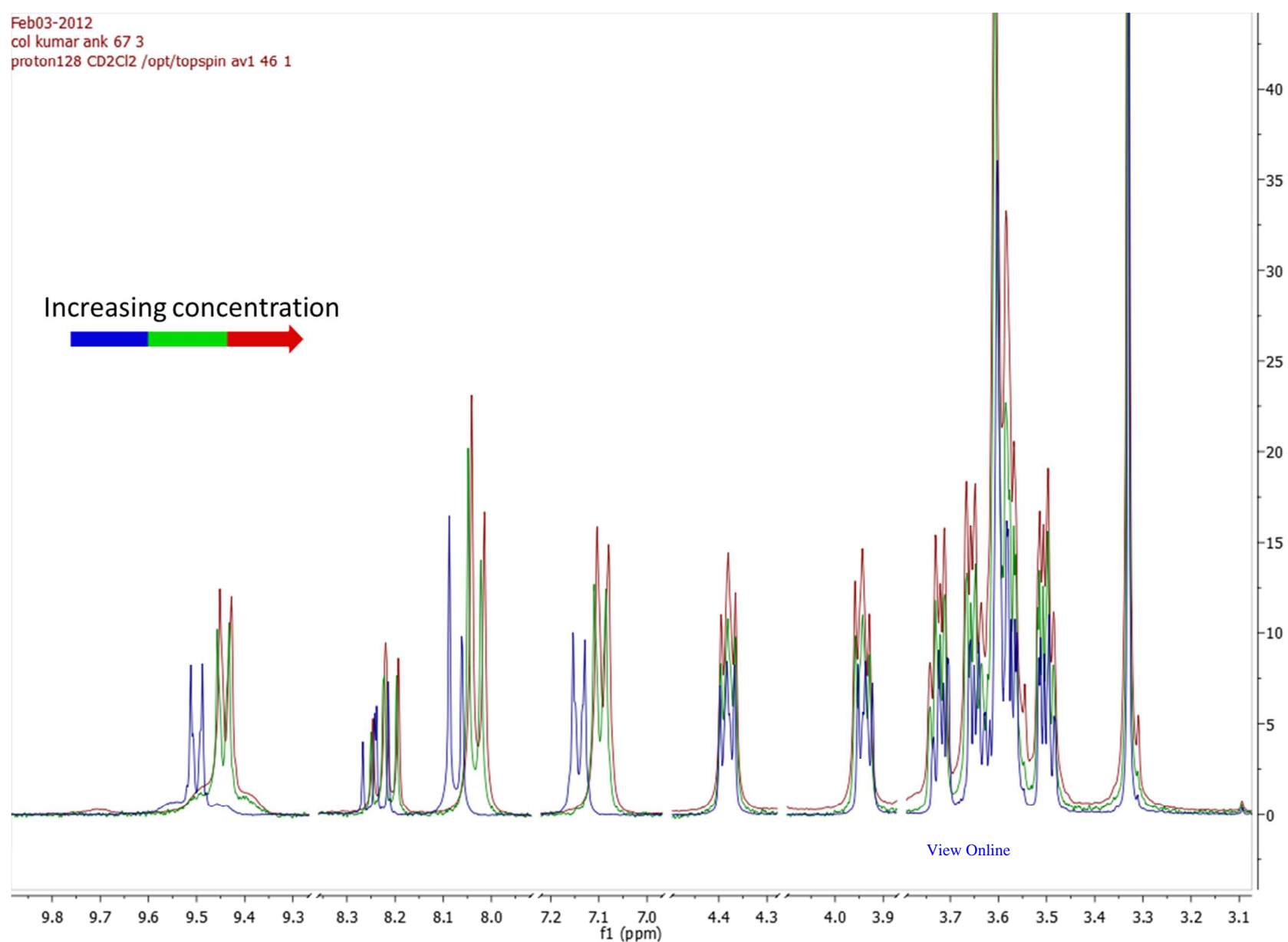


**Figure S2.** Concentration dependent  $^1\text{H}$ NMR ( $\text{CD}_2\text{Cl}_2$ , aromatic region) of complex **4** (blue 9.6 mM, green 19.2 mM and red 28.8mM).

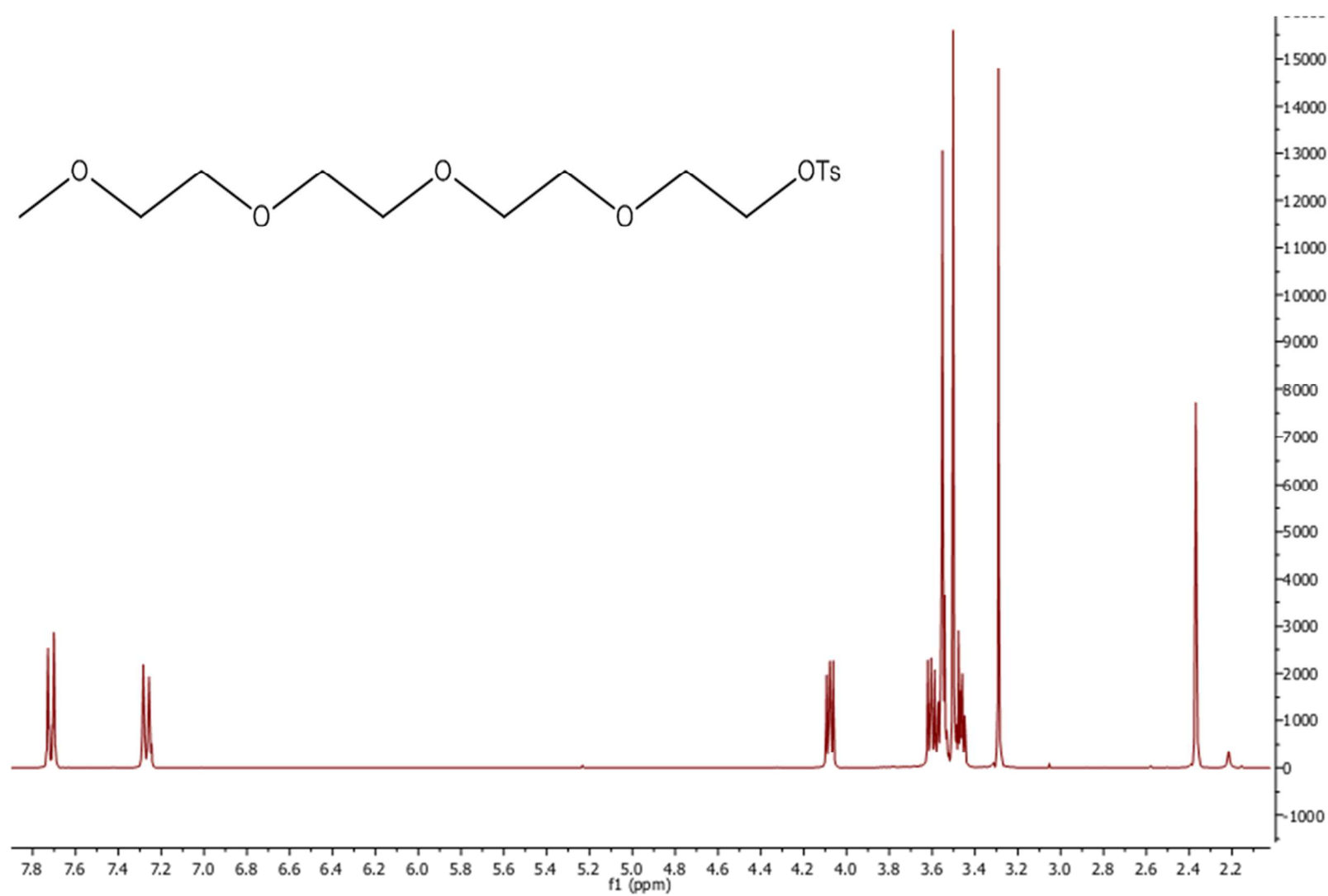


**Figure S3.**  $^1\text{H}$ NMR of compound **1** in  $\text{CDCl}_3$ .

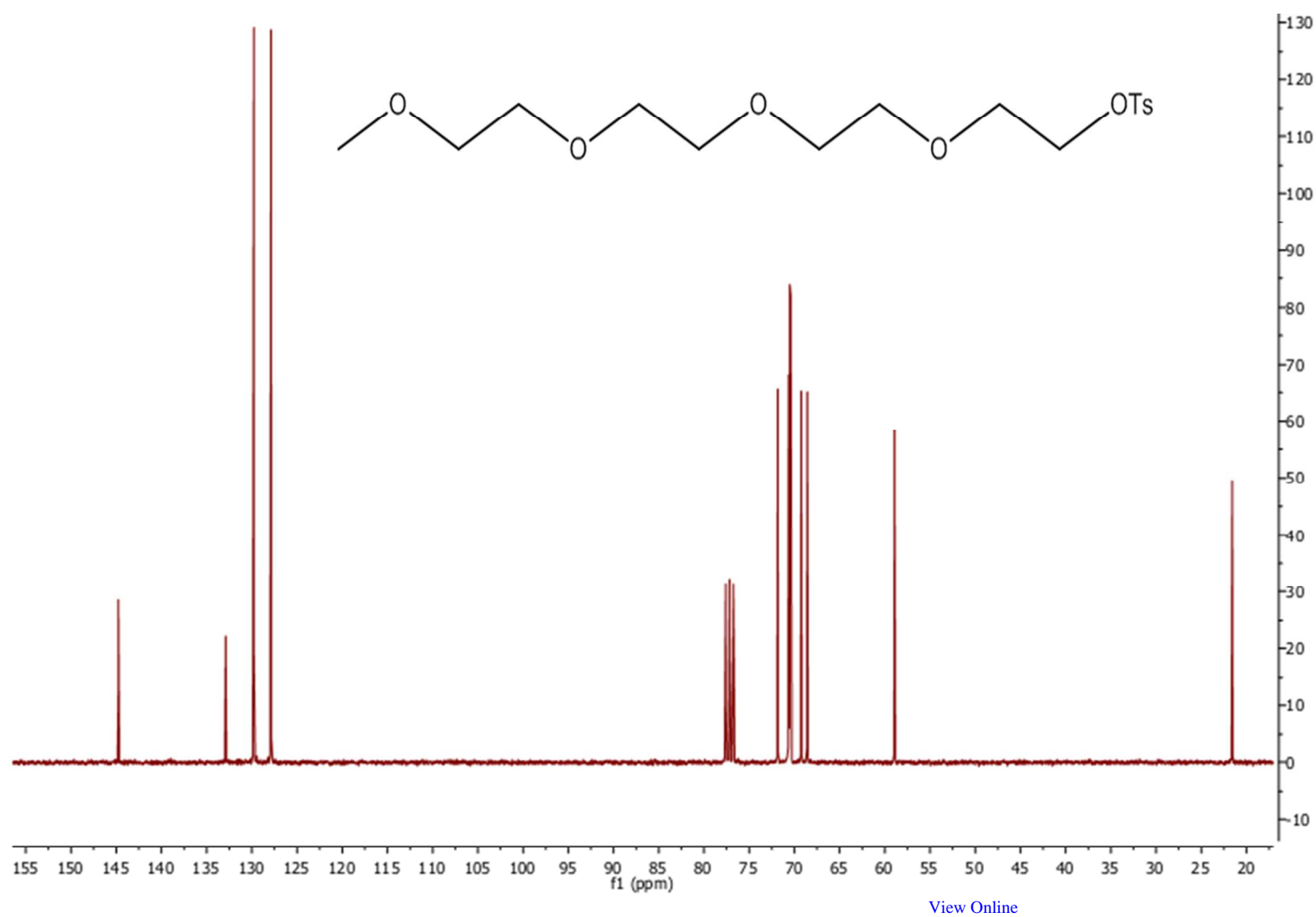


**Figure S4.**  $^{13}\text{C}$ NMR of compound **1** in  $\text{CDCl}_3$ .

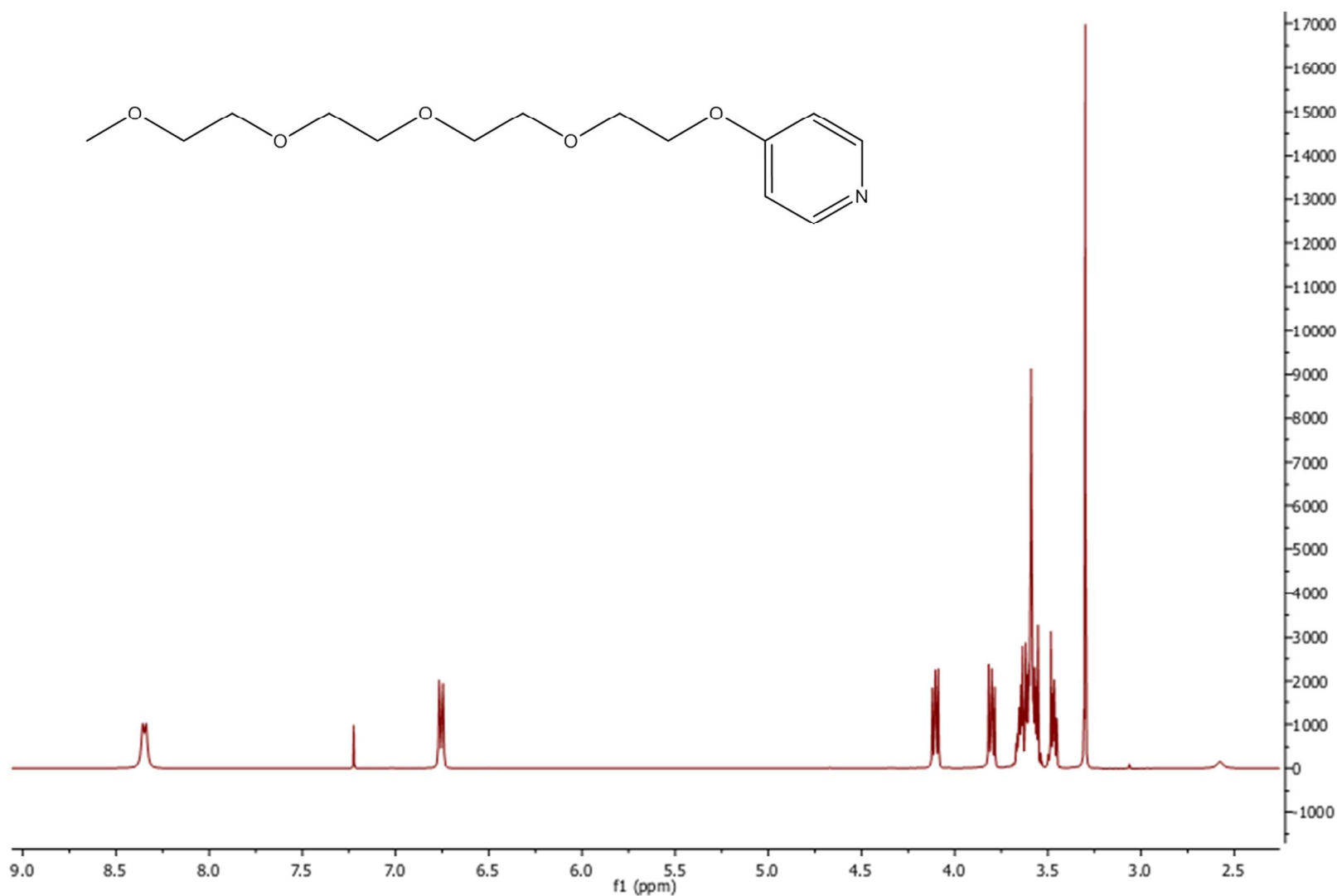


**Figure S5.**  $^1\text{H}$ NMR of compound **2** in  $\text{CDCl}_3$ .

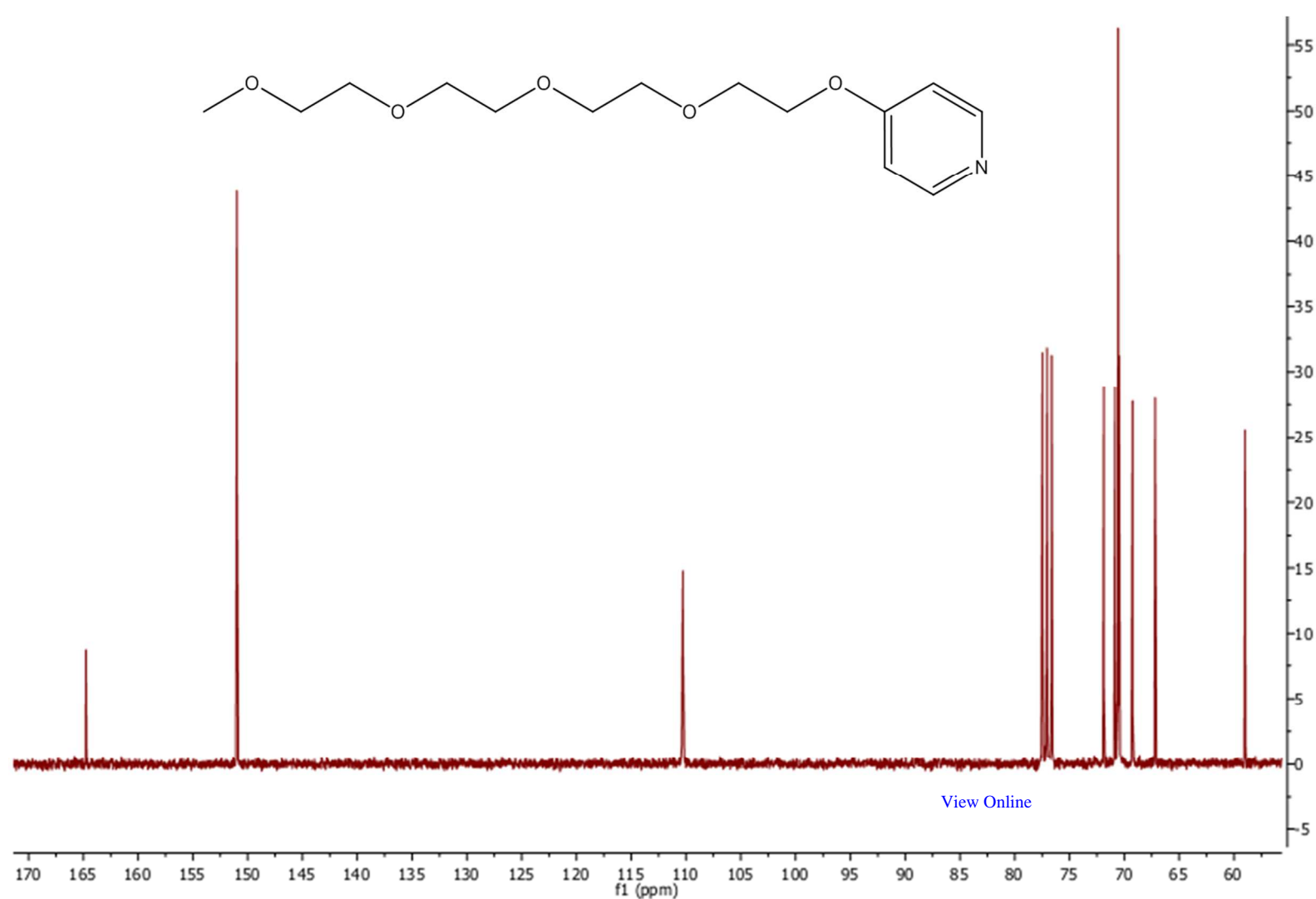


**Figure S6.**  $^{13}\text{C}$ NMR of compound **2** in  $\text{CDCl}_3$ .

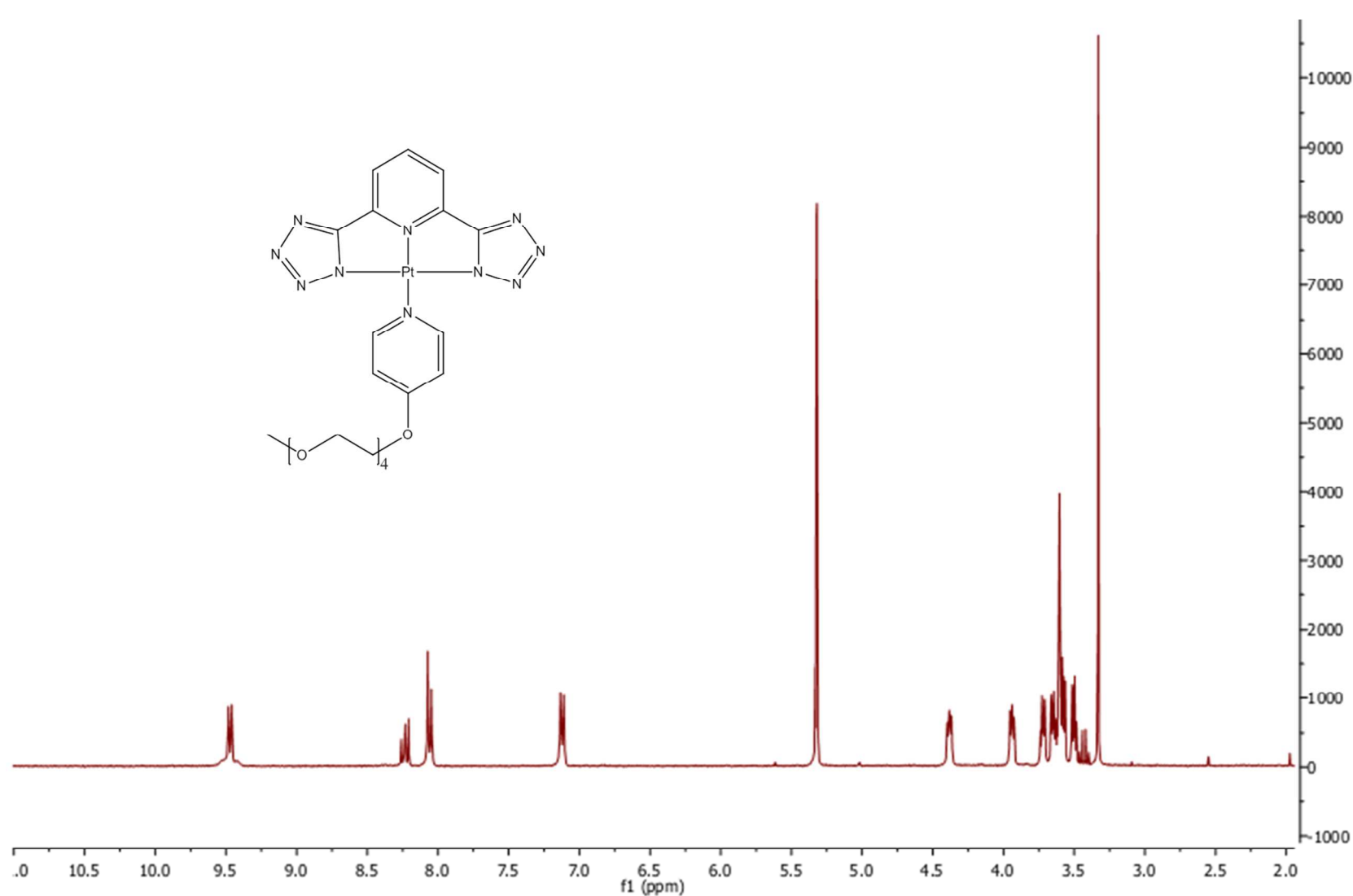


**Figure S7.**  $^1\text{H}$ NMR of complex **4** in  $\text{CD}_2\text{Cl}_2$ .